Biochimica et Biophysica Acta 1840 (2014) 1913–1922

Contents lists available at ScienceDirect

Biochimica et Biophysica Acta

journal homepage: www.elsevier.com/locate/bbagen

Synthesis and characterization of curcumin loaded polymer/lipid based nanoparticles and evaluation of their antitumor effects on MCF-7 cells

Sathish Sundar Dhilip Kumar [a], Ayyavu Mahesh [b], Surianarayanan Mahadevan [a,*], Asit Baran Mandal [a]

[a] Thermochemical Lab, Chemical Engineering Department, Central Leather Research Institute, Chennai 600 020, India
[b] School of Biological Sciences, Madurai Kamaraj University, Madurai 625 021, India

ARTICLE INFO

Article history:
Received 9 October 2013
Received in revised form 7 January 2014
Accepted 10 January 2014
Available online 16 January 2014

Keywords:
Polyhydroxyethyl methacrylate
Stearic acid
Curcumin
Drug delivery system
Polymeric lipid nanoparticle

ABSTRACT

Background: Hybrid materials are synthesized using hydrophilic polymer and lipids which ensure their long term systemic circulation through intravenous administration and enhance loading of hydrophobic drugs. The purpose of this study is to prepare, characterize and evaluate the in vitro efficacy of curcumin loaded polyhydroxyethyl methacrylate/stearic acid nanoparticles in MCF-7.
Methods: C-PSA-NPs, prepared using the emulsification–solvent evaporation method were characterized by dynamic laser scattering, SEM, AFM, FT-IR, X-ray diffraction, and TGA. The in vitro release behavior was observed in PBS pH 7.4, the anticancer potential was analyzed by MTT assay, cell cycle and apoptosis studies were performed through flow cytometry. C-PSA-NPs drug localization and cancer cell morphological changes were analyzed in MCF-7 cell line.
Results: C-PSA-NPs exhibited the mean particle size in the range of 184 nm with no aggregation. The surface charge of the material was around −29.3 mV. Thermal studies (TGA) and surface chemistry studies (FT-IR, XRD) showed the existence of drug curcumin in C-PSA-NPs. The MTT assay indicated higher anticancer properties and flow cytometry studies revealed that there were better apoptotic activity and maximum localization of C-PSA-NPs than curcumin.
Conclusions: Polymer lipid based drug delivery appeared as one of the advancements in drug delivery systems. Through the present study, a novel polymer lipid based nanocarrier delivery system loaded with curcumin was demonstrated as an effective and potential alternative method for tumor treatment in MCF-7 cell line.
General significance: C-PSA-NPs exhibited potent anticancer activity in MCF-7 cell line and it indicates that C-PSA-NPs are a suitable carrier for curcumin.

1. Introduction

Nanotechnology is the term commonly used now to refer to the fabrication of new materials such as "solid colloidal particles" with nanoscale dimensions. In the field of drug delivery there has been substantial interest in developing nanoparticles as effective drug carriers, wherein the drug or biologically active material is entrapped, encapsulated, adsorbed or attached [1,2]. Polyhydroxyethyl methacrylate (PHEMA), a hydrophilic polymer is widely used as a drug carrier molecule [3,4]. The hydrogels are used in biomedical applications because of their distinctive biocompatibility like absence of toxicity and compatibility with blood [5–8]. Some of its applications include eye contact lenses, scaffold materials in tissue engineering, artificial skin, and tube-shaped structure grafts [9–12].

Curcumin (Diferuloylmethane), a low molecular weight, lipophilic, natural yellow polyphenolic compound of Indian spice turmeric (*Curcuma longa*), has the chemical structure of (1,7-bis(4-hydroxy-3-methoxyphenyl)-1,6-heptadiene-3,5-dione). It has been used in traditional medicine for many centuries in India and China [13–18]. It possesses a wide range of biological and pharmacological properties, and is used for the treatment of neurodegenerative, cardiovascular, pulmonary, autoimmune and neoplastic diseases [14], biliary disorders, hepatic disorders, diabetic wounds, rheumatism [16], and skin cancer [19] and it is an antioxidant, antiviral, and anticancer [20,21] showing anti-inflammatory drug properties [13,22,23]. Though curcumin has good therapeutic efficacy (topical & oral), the problem related to curcumin is its low solubility in aqueous solution, degradation at alkaline pH, photodegradation and its poor oral bioavailability [16,24,25]. Carrier mediated curcumin delivery is the potential way to overcome these problems without affecting its efficacy [26]. Recent research has concentrated on delivering curcumin [27] through different carrier molecules such as polymeric micelles, polymeric nanoparticles, liposomes, lipid based nanoparticles, hydrophilic polymers or hydrogels, and cyclodextrin.

Stearic acid (SA), an endogenous long-chain fatty acid is biocompatible with low toxicity. It is biocompatible with human tissues and neutral with relevance to physiological fluids. Lipids in combination with a

* Corresponding author at: Thermochemical Lab, Chemical Engineering Department, Central Leather Research Institute (CLRI), Adyar, Chennai 20, Tamilnadu, India. Tel.: +91 44 24437207; fax: +91 44 24911589.
E-mail address: msuri1@vsnl.com (S. Mahadevan).

0304-4165/$ – see front matter © 2014 Elsevier B.V. All rights reserved.
http://dx.doi.org/10.1016/j.bbagen.2014.01.016

hydrophilic polymer (in the assembly of nanoparticles) are found to possess excellent physical and chemical stability and hence provide protection against degradation of drugs [28]. Lipid mixtures have the ability to load hydrophobic, hydrophilic and alternative biomacromolecules like peptides and proteins [29,30]. Stearic acid (SA) has potential and is a well documented pharmaceutical excipient for anticancer drug delivery due to its ability to internalize in cancer cells and accumulate in cytoplasm [29,31].

The polymer/lipid based nanoparticles have not yet been explored as potential systems for the delivery of curcumin.

The present study focuses on synthesis and characterization of curcumin loaded PHEMA/stearic acid (C-PSA-NPs) conjoint based nanoparticles, through environmentally benign approaches. The efficacy of the synthesized nanoparticles is evaluated with MCF-7 cell line. The use of amphiphilic Pluronic F-68 [32] as an emulsifier and a stabilizer is investigated to understand the means to provide an apt drug delivery system for a hydrophobic drug like curcumin.

2. Materials and methods

2.1. Materials

Choline formate ionic liquid (IL) was synthesized as per reported procedure [33]. The purity and the presence of moisture in choline formate (CF) were verified by comparing the FT-IR and ^{1}H NMR standard spectra. HEMA (2-hydroxyethyl methacrylate) and curcumin (≥94%) were obtained from Sigma-Aldrich, Bangalore. Stearic acid and Pluronic F-68 were procured from Merck India Ltd., Bangalore. Stearic acid was purified by recrystallization from 95% ethanol.

MCF-7 cell line was obtained from the National Centre for Cell Science (NCCS), Pune, India. Minimum Essential Medium Eagle (MEM), 10% Fetal Bovine Serum (FBS), Trypsin–EDTA and penicillin (100 U/ml)/streptomycin (100 μg/ml) obtained from HiMedia, India, were used without further purification, for cell line studies. MTT (4,5-dimethyl thiazol-2,5-diphenyl tetrazolium bromide), dimethylsulfoxide (DMSO), and glycine buffer were obtained from Sigma-Aldrich, Bangalore. All other chemicals and reagents were of analytical grade. Double distilled water was used for all the experiments.

2.2. Preparation of curcumin loaded PSA nanoparticles (C-PSA-NPs)

The polymer matrix was synthesized using HEMA and IL (volume ratio: 1:1), and the mixture was poured into polystyrene plate and kept in a dessicator; it was exposed to nitrogen for 24 h [33,34]. Curcumin loaded PSA nanoparticles (C-PSA-NPs) were prepared by emulsification–solvent evaporation method [35]. Precisely, 200 mg of polymerized PHEMA gel was dissolved in a binary solvent (acetone and ethanol in the ratio of 4:1) with 50 mg of SA and curcumin. The mixture was stirred for 10 min in a magnetic stirrer (IKA, Germany). The above mixture was added drop by drop in an aqueous solution of 1% of Pluronic F-68 (w/v), simultaneously homogenizing at 15,000 rpm for 3 min using Homogenizer (IKA, Germany), to form an emulsion. Subsequently, the organic solvent was evaporated by stirring the emulsion for 8 h at 40 °C until the formation of C-PSA-NPs. The nanoparticle suspension was then dispensed into 10 ml vials and transferred to a VirTis freeze-dryer (New York, USA). After the drying process that lasted for 48 h at −70 °C, the lyophilized powder was stored. The control sample of PSA-NPs (without curcumin) was synthesized by adopting the above procedure.

2.3. Hemocompatibility assay

Hemolysis assay was performed to test the hemocompatibility of the PSA-NPs by studying the effect of nanoparticles on erythrocytes. Heparinized buffer (1 mg of heparin in 500 ml of PBS (pH 7.4)) was used in the experiment. RBC suspension was prepared by diluting 1 ml of human blood to 10 ml using heparinized buffer. To find the optimum concentration of RBC needed for study, different quantities of RBC suspension were incubated with distilled water, and centrifuged; the supernatant was analyzed using UV spectrophotometer. The RBC concentration corresponding to optimum O.D. value of 0.49 was used for further studies. Various concentrations of the PSA-NPs were mixed with optimized volume of RBC suspension and the volume was made up to 1 ml using heparinized buffer. Distilled water with RBC suspension was treated as a positive control and heparinized buffer with RBC suspension served as a negative control. The samples were incubated at room temperature for 30 min, followed by centrifugation for 10 min at 4 °C. The absorbance of the supernatant was read at 540 nm. The percentage hemolysis was calculated using Eq. (1).

$$\text{Hemolysis}(\%) = \frac{[(\text{Absorbance of sample}) - (\text{Absorbance of blank})]}{\text{Absorbance of positive control}} \times 100. \quad (1)$$

2.4. Loading efficiency and solubility study of curcumin

In order to determine the loading efficiency of curcumin (%) in C-PSA-NPs, UV–vis spectrophotometer (Shimadzu UV 2101 PC) studies at 426 nm were carried out. A standard curve in the range of 2–10 μg curcumin was plotted. The curcumin content present in C-PSA-NPs was calculated as loading efficiency using Eq. (2). Aqueous solubility of curcumin and C-PSA-NPs was determined by dissolving separately in 0.01 M of PBS in pH 7.4.

$$\text{Loading efficiency}(\%) = \frac{\text{amount of curcumin loaded in C-PSA-NPs}}{\text{amount of curcumin intially added}} \times 100. \quad (2)$$

2.5. Physicochemical characterization

2.5.1. Particle size and zeta potential measurements

Particle size distribution and zeta potential of the C-PSA-NPs were studied by photon correlation spectroscopy (Zetasizer ver 6.00, Malvern Instruments Ltd., UK). For light scattering experiments, the samples were measured at a fixed angle of 90° at 25 °C. The scattering intensity was adjusted in the range of 50–500 kcps by diluting the sample with deionized water. All measurements were carried out in triplicate.

2.5.2. Morphological examination

Morphological studies of C-PSA-NPs were performed with scanning electron microscope (JEOL SEM model JSM 5610 LV). A drop of C-PSA-NPs suspension was placed on a graphite surface and allowed to dry completely as C-PSA-NPs were coated with gold by ion sputter. The coating was performed at 20 mA for 4 min and then images were recorded. The shape and surface morphology of C-PSA-NPs were further analyzed by Atomic Force Microscopy (Park Systems XE-70, South Korea). A drop of diluted nanoparticle suspension was placed on freshly cleaved mica. After a minute of incubation the surface was gently rinsed with deionized water to remove unbound nanoparticles. The sample was air dried at room temperature (25 °C) and mounted on the microscope scanner. The image processing was done using XEL software.

2.5.3. Fourier transform infrared spectroscopy

Fourier transform infrared (FT-IR) spectra were obtained on a PerkinElmer 1000 paragon FT-IR spectrometer. The spectra were recorded in the region of 400–4000 cm^{-1} (resolution of 1 cm^{-1}) for KBr pellets of curcumin, PSA-NPs and C-PSA-NPs.

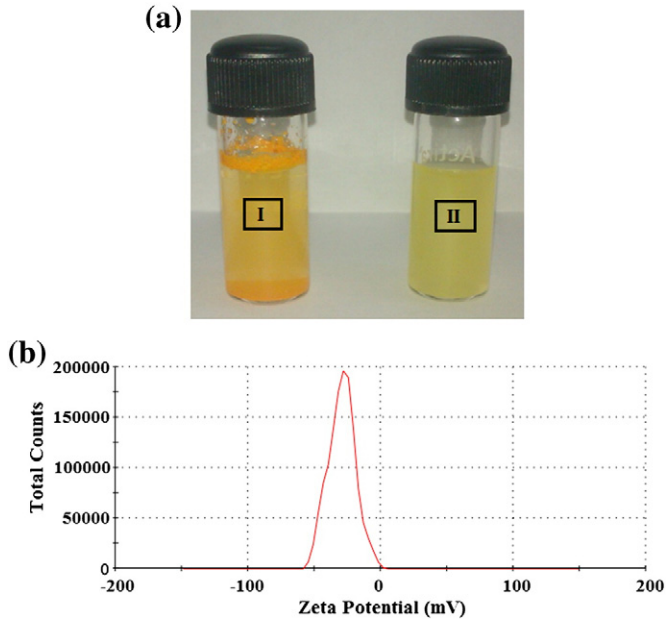

Fig. 1. [a] Photographs showing the comparative solubility of curcumin and C-PSA-NPs in PBS [I. Curcumin & II. C-PSA-NPs in PBS (0.01 M, pH 7.4)]; [b] zeta potential of C-PSA-NPs by using dynamic laser scattering.

2.5.4. X-Ray diffraction (XRD) study

XRD analysis was done to study the crystallographic structure of the C-PSA formulation. The patterns of curcumin, PSA-NPs and C-PSA-NPs were obtained using X-ray diffractometer (PANalytical X'Pert Powder XRD System). The measurements were performed at a voltage of 40 kV and 25 mA. The scanned angle was set from $10° \leq 2° \geq 70°$ and the scan rate was 2 min^{-1}.

2.5.5. Thermal analysis

In order to understand the thermal behavior of nanoparticles, curcumin, PSA-NPs, and C-PSA-NPs were subjected to thermal gravimetric analysis (TGA Q50 V20.6 Build 31, Universal V 3.9A TA instruments). The sample of 5 mg was placed on a thin platinum pan and the measurement was conducted at a heat flow rate of 10 °C min^{-1} under nitrogen purging. The temperature range of measurement was between 30 and 600 °C.

2.5.6. In vitro release studies

The in vitro release studies of curcumin from C-PSA-NPs were performed using a dialysis bag method. C-PSA-NPs were suspended in 5 ml of PBS (pH 7.4) containing 1% v/v Tween-80 and the dialysis bag was placed in 35 ml of PBS, and kept under stirring (100 rpm) at 37 °C [36,37]. The sample (1 ml) was withdrawn at predetermined intervals to estimate released curcumin. Then equal volume of fresh buffer was added to maintain sink conditions. The released curcumin was determined spectrophotometrically at 426 nm. The concentration of released drug was then calculated using a standard plot pre-drawn in the range of 2–10 μg. The percentage of curcumin released was determined from the following equation.

$$\text{Release}(\%) = \frac{\text{Released Curcumin}}{\text{Total Curcumin}} \times 100. \quad (3)$$

2.6. In vitro cytotoxicity studies

The standard MTT assay was used to determine the cytotoxicity of C-PSA-NPs using MCF-7 cells. MCF-7 cells were grown in MEM media supplement, with 10% FBS and 1% antibiotic penicillin/streptomycin mixture. MCF-7 cells were seeded on 96-well plates and incubated at 37 °C in a humidified atmosphere of 5% CO_2. On reaching 80% adherent confluency, cells were treated with a range of concentrations at 2, 5, 10, 15, 20, 25, 30, & 50 μg/ml of curcumin, PSA-NPs and C-PSA-NPs and

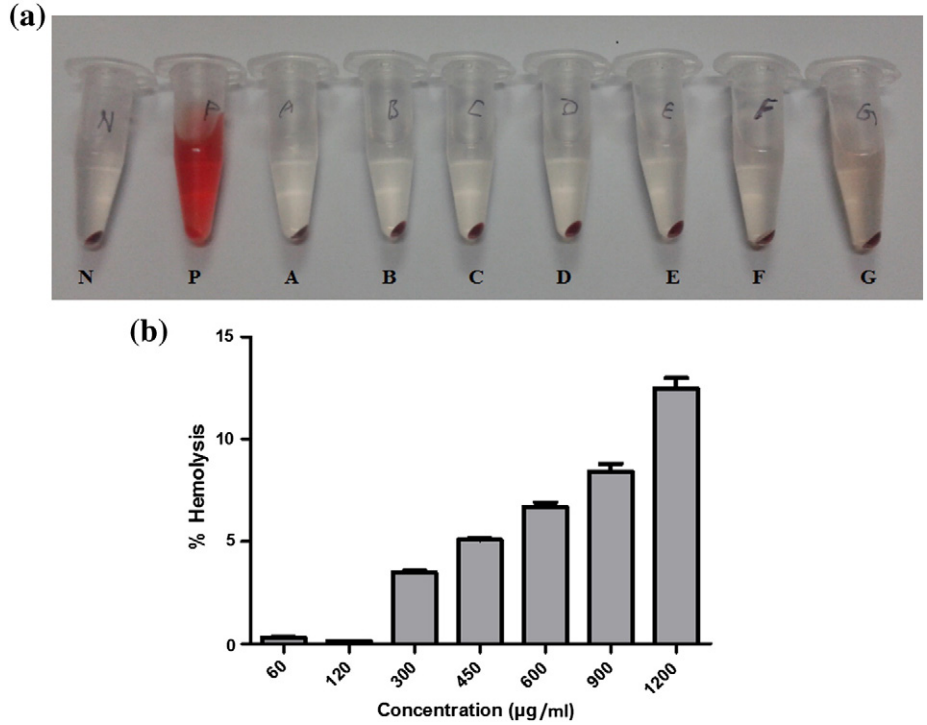

Fig. 2. [a] Images showing blood compatibility of PSA-NPs [N—Negative control, P—Positive control, A—60 μg/ml, B—120 μg/ml, C—300 μg/ml, D—450 μg/ml, E—600 μg/ml, F—900 μg/ml, G—1200 μg/ml]; [b] hemocompatibility study; percentage hemolysis of PSA-NPs in the concentration ranges of 60–1200 μg/ml.

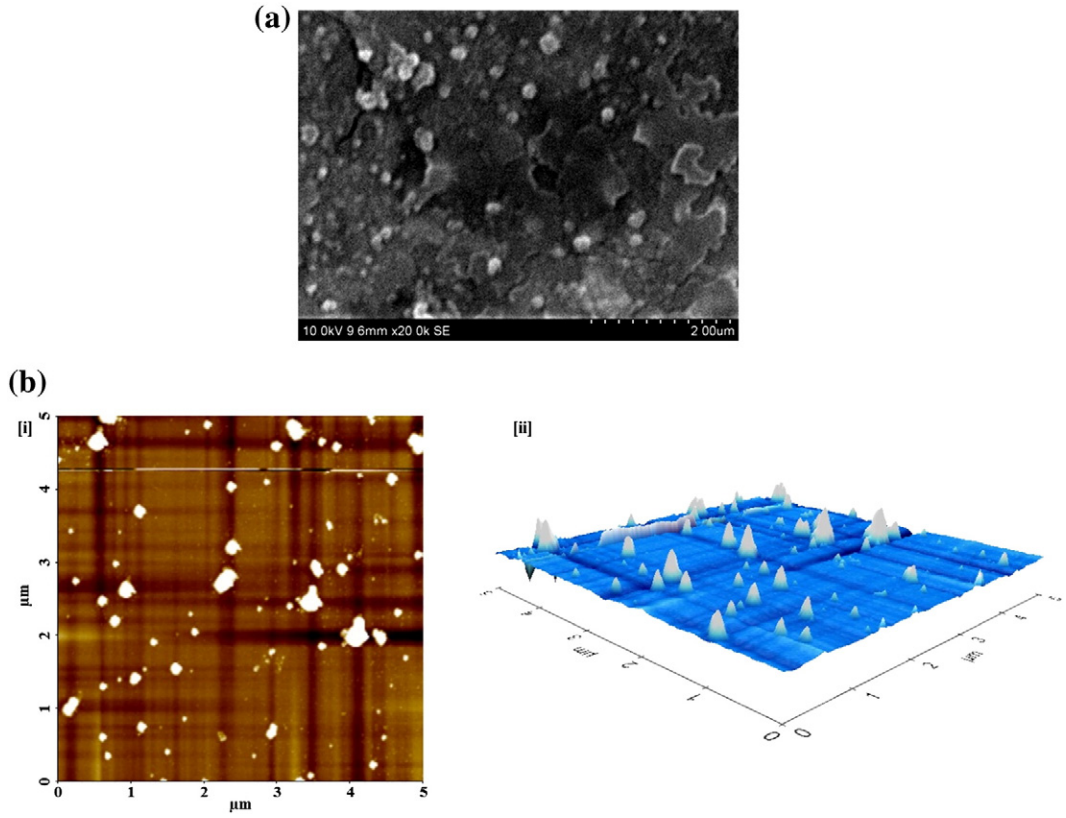

Fig. 3. [a] SEM image of C-PSA-NPs; [b] [i] AFM images of C-PSA-NPs and [ii] three dimensional view.

incubated for 48 h. The untreated cells and neat PSA-NPs were kept as control and blank respectively. After this, 200 µl of MTT was added and the plates were incubated at 37 °C, 5% CO_2 for 4 h. The absorbance was read at 570 nm. The cytotoxicity (IC_{50}) is calculated based on the color yield of treated cells which is proportional to the number of metabolically active cells and indirectly approximates cell viability. IC_{50} is defined as the drug concentration required to inhibit growth of cells by 50% relative to control (IC_{50}). A graph was drawn using % of cell viability with respect to the concentration of the sample.

2.7. Cell cycle analysis

For cell cycle analysis, 1×10^6 MCF-7 cells were seeded in 6-well plates and grown in MEM (HiMedia, India) supplemented with 10% FBS for 24 h under standard cell culture conditions. Then cells were treated with the PSA-NPs, curcumin, and C-PSA-NPs and untreated cells served as control for 48 h. Trypsinized cells were washed twice with PBS and then the cells were suspended again in PI staining solution (50 µg/ml propidium iodide, 200 µg/ml DNase free RNase, 4 mM sodium citrate, 0.1% Triton X-100) and incubated for 15 min in dark. The experiment was performed in flow cytometry (BD FACSAria III, BD Biosciences, USA). FlowJo software was used for data analysis and to discriminate the cell cycle phases.

2.8. Apoptosis analysis by flow cytometry

Flow cytometry analysis of apoptosis was performed in Annexin V-PE/7-Amino-Actinomycin (7-AAD) dual stained MCF-7 cells. The staining was carried out using the PE Annexin V Apoptosis Detection Kit (BD Pharmingen™, US) as per the manufacturer's instructions. Annexin V-PE binds to phosphatidylserine in the membrane of cells when the apoptotic process begins, and the binding of 7-AAD to the cellular DNA in cells indicates late-apoptotic or necrotic cell death. Here, the cells were

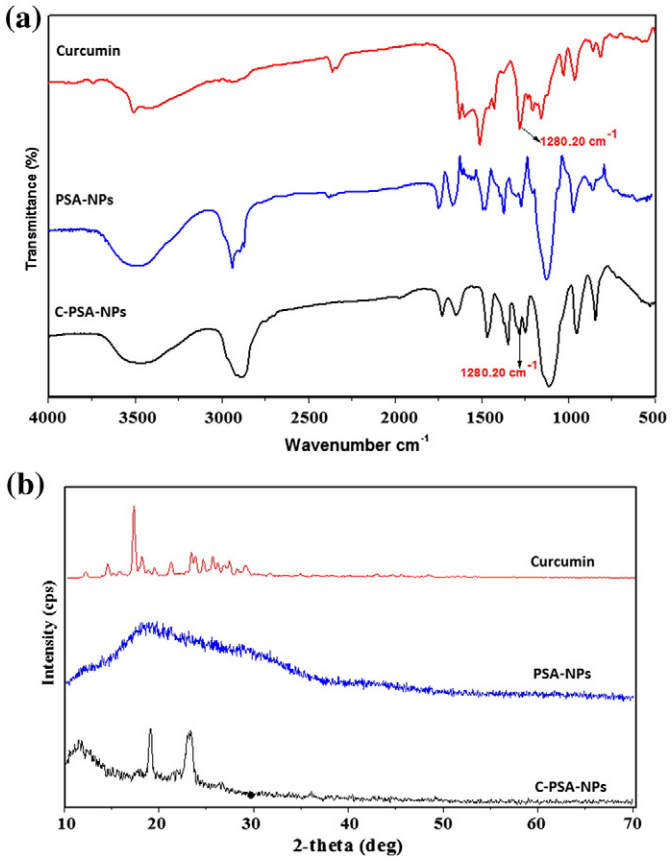

Fig. 4. [a] FTIR spectra of curcumin, PSA-NPs, and C-PSA-NPs; [b] XRD patterns of curcumin, PSA-NPs, and C-PSA-NPs.

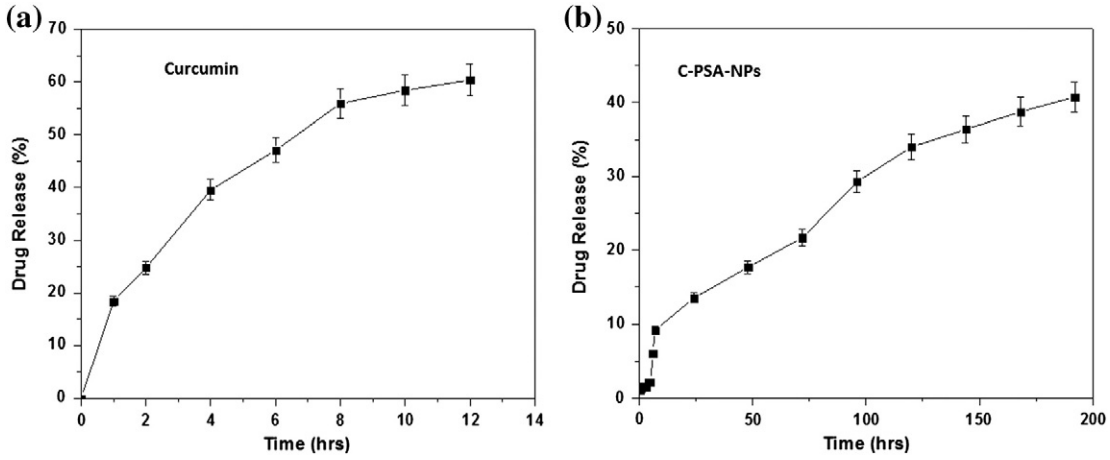

Fig. 5. In vitro release profile of [a] curcumin and [b] curcumin from C-PSA-NPs; in PBS at pH 7.4 (mean ± SD, n = 3).

treated with IC_{50} concentration of curcumin, PSA-NPs, and C-PSA-NPs for 48 h, and then the cells were taken to trypsinization and washed twice with ice-cold PBS. They were finally suspended in 1× binding buffer (100 mM HEPES/NaOH, pH 7.5 containing 1.4 M NaCl and 25 mM $CaCl_2$) at a concentration of 1×10^6 cells/ml. Five microliters of Annexin V-PE and 7-AAD was added in 100 μl of each cell suspension. The samples were mixed gently and incubated at room temperature for 15 min in the dark. After incubation, 400 μl of ice-cold 1× binding buffer was added and mixed gently and the percentage of apoptotic cells in the population was determined.

2.9. High content imaging

Localization of C-PSA-NPs and the cytotoxic effect were investigated in MCF-7 cell line. Briefly, 2×10^4 cells/well of MCF-7 cancer cell line were seeded on 96-well Cell Carrier microplates (PerkinElmer, US). When the cells reached 80% confluence the media were changed and then the cells were treated with PSA-NPs, curcumin and C-PSA-NPs and the plate was incubated for 24 h in humidified incubator at 37 °C with 5% CO_2. The cells were washed twice with ice cooled PBS and the drug was localized in live cells using Operetta High Content Imaging System (PerkinElmer, US).

3. Results and discussion

3.1. Preparation and characterization of PSA and C-PSA nanoparticles

As reported earlier [29], PHEMA gel was synthesized using choline formate ionic liquid, and PSA-NPs were prepared using optimized concentrations of polymer (PHEMA), lipid (stearic acid) and emulsifier (Pluronic F-68) by emulsification–solvent evaporation method. Polymer PHEMA concentration was fixed throughout the study and concentrations of both lipid and emulsifier were different. Of the three lipid concentrations studied (50, 75 and 100 mg), the nanoparticles were found to be stable and homogenous with no aggregation, at 50 mg of lipid concentration. (At 75 and 100 mg lipid concentrations, the nanoparticles obtained were found to be more aggregated leading to unstable dispersions with increased mean diameters of PSA-NPs.) A similar study was performed by varying Pluronic F-68 concentration (0.5, 1, and 2%) in aqueous solution. 1% Pluronic F-68 concentration provided PSA-NPs in the desired size range of around 184 nm. Curcumin loaded PSA nanoparticles (C-PSA-NPs) were prepared using optimum concentration of lipid (50 mg) and emulsifier (1%).

Drug loading efficiency was found to be 53.2%. The high drug loading was believed to be due to the incorporation of stearic acid in the formulation enabled better entrapment of hydrophobic drug curcumin. Solubility of curcumin and C-PSA-NPs was also determined by dissolving both curcumin and C-PSA-NPs into the aqueous solution and compared (Fig. 1a). It revealed that C-PSA-NPs were completely dissolved and a clear yellow well dispersed liquid could be seen. The average particle size, determined using DLS, was found to be 184 nm (Electronic

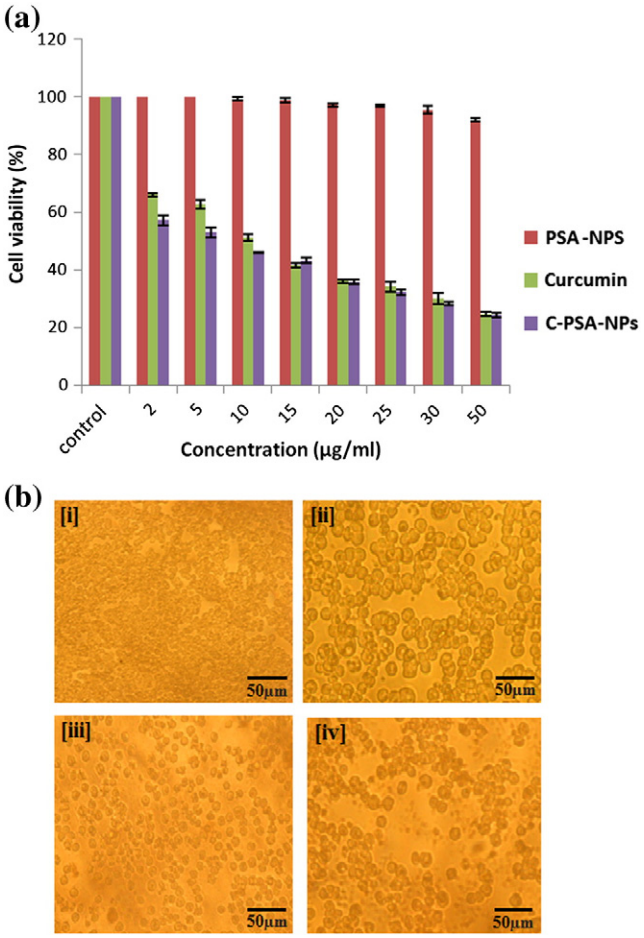

Fig. 6. [a] In vitro cytotoxicity studies (MTT assay) of curcumin, PSA-NPs and C-PSA-NPs in MCF-7 cell line; [b] images of MCF-7 cell line visualized under inverted microscope. [i] Control, [ii] PSA-NPs, [iii] curcumin, & [iv] C-PSA-NPs.

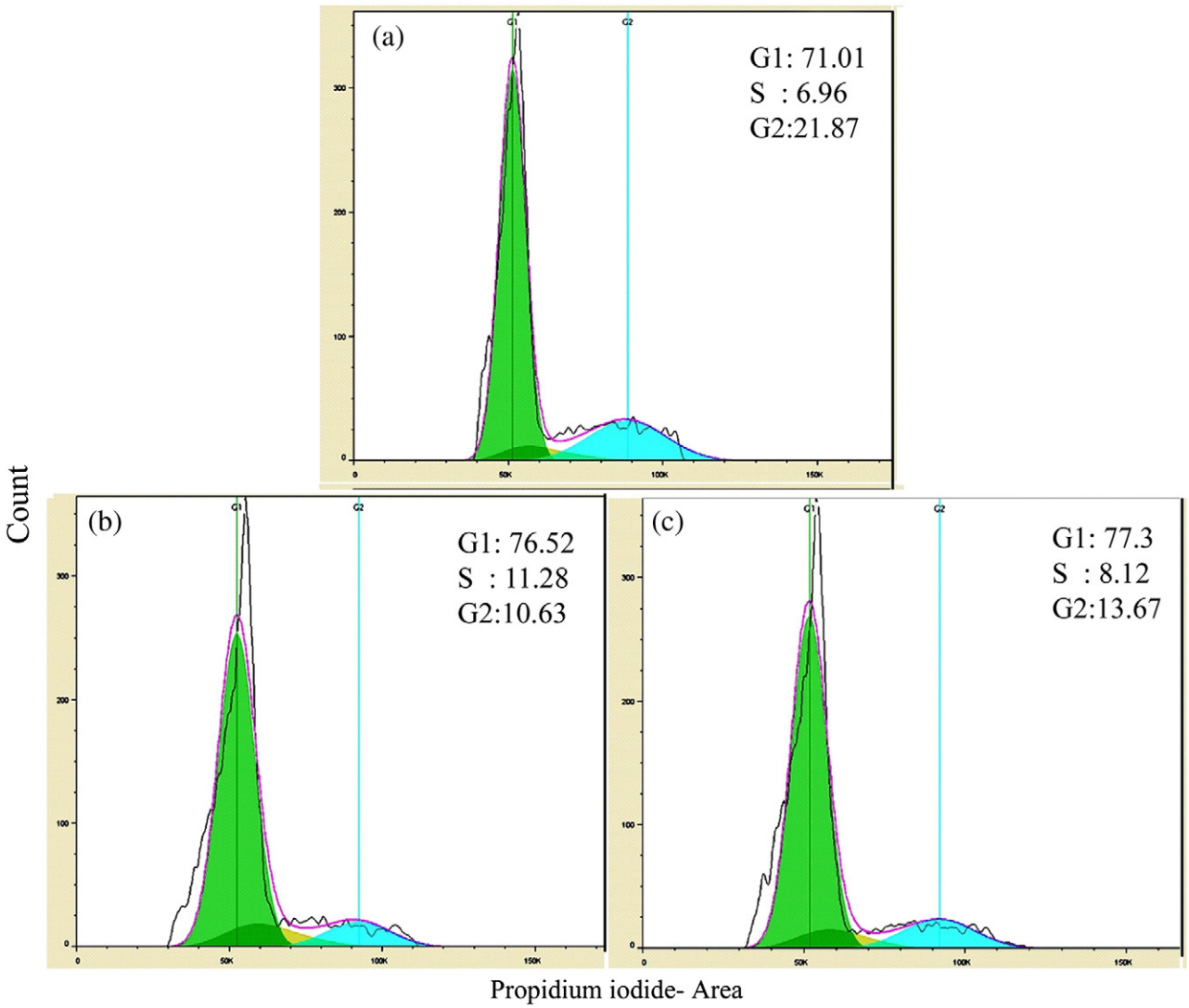

Fig. 7. The effect of C-PSA-NPs on the cell cycle analysis in MCF-7 cell line using flow cytometry [a] control, [b] curcumin, [c] C-PSA-NPs.

Supplementary Material I). Zeta potential measurement showed the surface potential of C-PSA-NPs to be −29.3 mV (Fig. 1b).

Thus, curcumin loaded polymer lipid nanoparticles, C-PSA-NPs, could be successfully synthesized with desired particle size and zeta potential. The increased drug loading efficiency in the present study (in contrast to one of the previous study [38]) could be attributed to the role of the lipid SA. The conjoint effort of incorporating curcumin in SA and PHEMA (C-PSA-NPs) appeared to be more promising due to the potential of long term systemic circulation of the hydrophilic polymer and lipid prepared with the use of copolymer non-ionic surfactants (Pluronic F-68) as emulsifiers [47]. The idea of incorporation of SA with PHEMA to achieve high drug loading of hydrophobic drug curcumin is found to be promising.

3.2. Hemocompatibility assay

The blood compatibility of synthesized nanoparticles is a significant criterion for biomedical and pharmaceutical applications [25]. In the present study, biocompatibility of synthesized PSA-NPs was evaluated using in vitro hemocompatibility assay. The results (Fig. 2a) showed the effect of concentrations of PSA-NPs on erythrocytes or total blood hemoglobin. The percentage of hemolysis was found to be the lowest (Fig. 2b). The C-PSA-NPs showed moderate level of compatibility with blood cells. The results corroborated with previously published work of Chouhan and Bajpai [10].

3.3. Thermogravimetric analysis

TGA studies of curcumin, PSA-NPs, and C-PSA-NPs were carried out to assess their thermal behavior. Degradation of curcumin, PSA-NPs, and C-PSA-NPs with increasing temperature was shown (Electronic Supplementary Material II). The study confirmed that PSA-NPs were stable up to a temperature of 150 °C; however, C-PSA-NPs showed an increase in stability up to a temperature of 370 °C. A close observation of the TGA curve revealed that PSA nanoparticles underwent a two step degradation, first in the range of 150 to 280 °C showing a weight loss of 58%, and the second in the range of 280 to 400 °C with further degradation of PSA-NPs and a weight loss of 42%. The first step degradation was presumably due to the loss of SA as confirmed from the TGA curve of pure SA [39]. This trend confirmed the incorporation of SA in the PSA-NPs and low stability of PSA-NPs as compared to C-PSA-NPs.

3.4. Morphological study

The SEM image shown in Fig. 3a revealed that the particles were spherical in shape with monodispersed size distribution in the range of ~200 nm size, corroborating DLS studies. Further the morphological

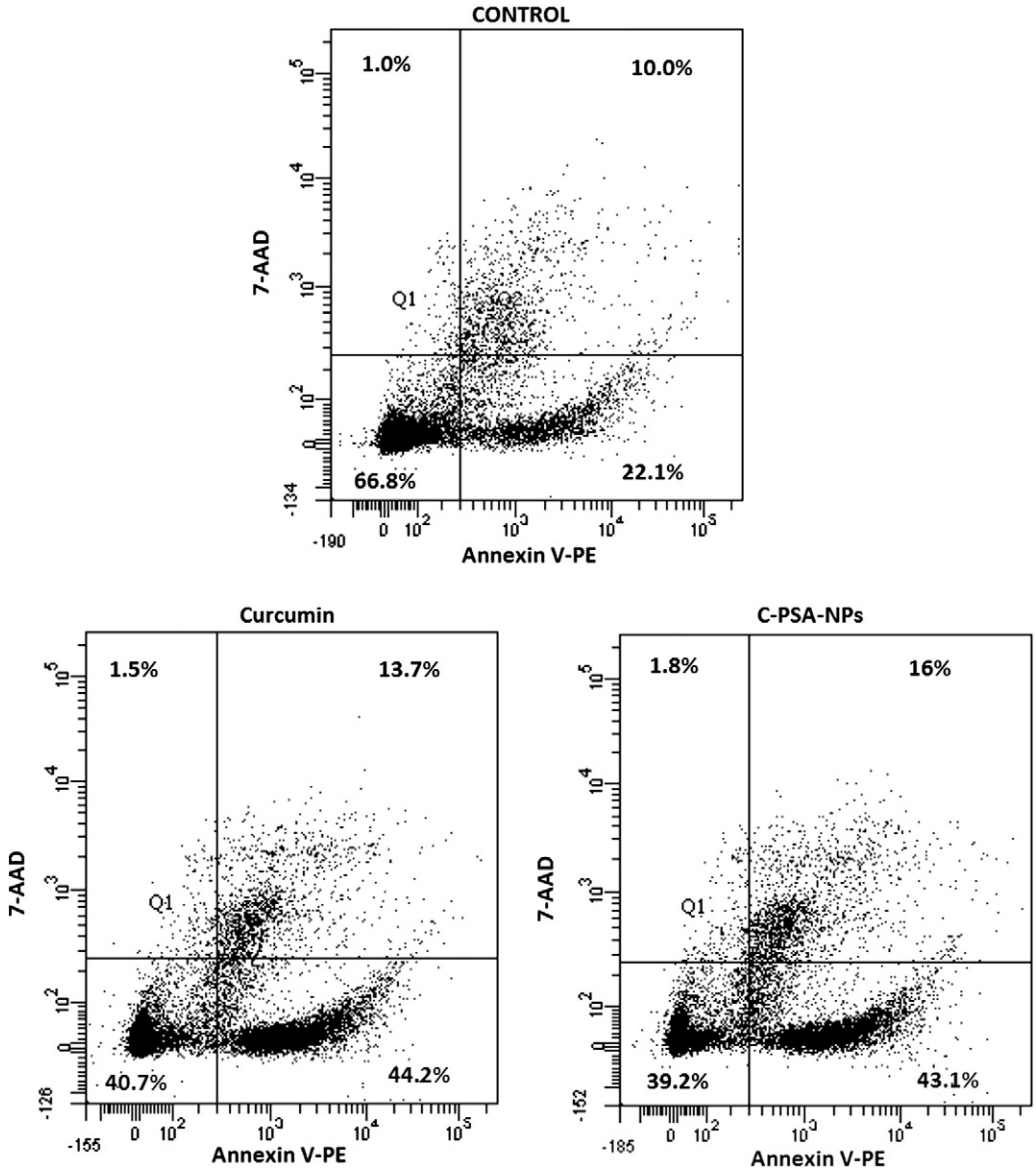

Fig. 8. Flow cytometry detection of necrotic, early, and late apoptosis in MCF-7 cell line treated with curcumin and C-PSA-NPs.

information of C-PSA-NPs was investigated using AFM and images are shown in Fig. 3b. The results confirmed that the particles were spherical in shape, without any aggregation [40].

3.5. FTIR study

FTIR spectra of curcumin, PSA-NPs and C-PSA-NPs are shown in Fig. 4a. In both PSA-NPs and C-PSA-NPs, the characteristic peaks of PHEMA were noticed at 3460–3560 cm^{-1} due to the hydrogen bonded O–H stretching, 1728 cm^{-1} C═O stretching, 1172 cm^{-1} O–C–C stretching, 2951 cm^{-1} asymmetric stretching of methylene group and 1454 cm^{-1} O–H bending, respectively. The results were in agreement with the previous studies of Chouhan and Bajpai [9]. A close observation of FTIR spectra of the samples PSA-NPs and C-PSA-NPs indicated the presence of stearic acid in the peak range of 2850–2960 cm^{-1} corresponding to CH stretching of aliphatic hydrocarbon [41]. The peak observed at 1280.6 cm^{-1} in the curcumin loaded C-PSA-NPs confirmed the aromatic C–O stretching vibrations of curcumin and the bands from 1280 to 1114 cm^{-1} marked the presence of C–O stretching [42]. FTIR spectra confirmed the incorporation of curcumin in the C-PSA-NPs.

3.6. X-Ray diffraction study

X-Ray diffraction studies were carried out for PSA-NPs, C-PSA-NPs and curcumin to understand the nature of curcumin in C-PSA-NPs (Fig. 4b). The characteristic peak of curcumin was observed in the 2-theta range of 10–30 °C, indicating the high crystalline nature of curcumin. However, the significant peaks of curcumin were absent in C-PSA-NPs. This absence of functional peaks of curcumin in C-PSA-NPs indicated the amorphous nature of curcumin or disordered crystalline phase. A similar phenomenon was reported earlier [40,43,44]. So the X-ray diffraction studies confirmed the desired amorphous nature of C-PSA-NPs.

3.7. In vitro release study

In order to obtain quantitative and qualitative information on drug release from the C-PSA-NPs, the release profile was determined by an in vitro dialysis method. Fig. 5a & b demonstrates the release profile of curcumin and C-PSA-NPs. Sustained release of curcumin was observed from C-PSA-NPs over a period of 8 days. A comparative release pattern

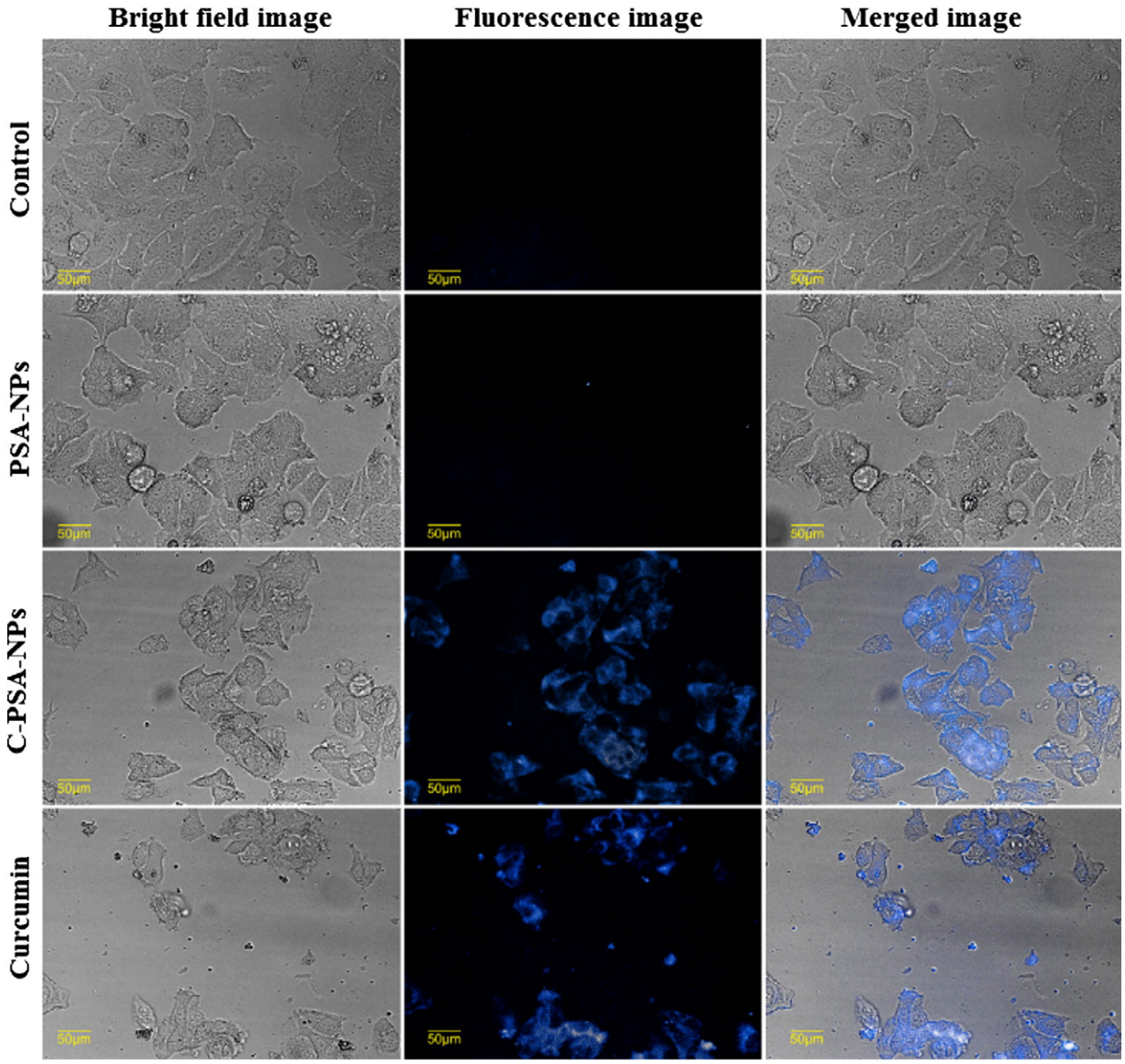

Fig. 9. Drug localization studies of control, curcumin, PSA-NPs and C-PSA-NPs in MCF-7 cell line.

of the C-PSA-NPs and curcumin in the first 12 h revealed that there was only a 10% release noticed from C-PSA-NPs, whereas curcumin exhibited a release of up to 60%. Thus the initial release in the first 12-h period could not be treated as a burst release in comparison to the curcumin release. The sustained release of C-PSA-NPs (40%) during the period of 8 days indicated its applicability as a drug delivery system [36].

3.8. In vitro cytotoxicity study (MTT assay)

MCF-7 cells were used to evaluate the anticancer activity of curcumin, PSA nanoparticles and C-PSA-NPs. The cell viability was studied by a standard MTT assay [45]. The untreated cells and PSA-NPs were kept as control and blank respectively. The assay was terminated at 48 h and colorimetric determination of cell viability was performed using ELISA Reader (Qualigens, Bangalore, India). (The results are shown in Fig. 6a & b.) The IC_{50} concentrations of curcumin and C-PSA-NPs were 10.72 μg/ml and 7 μg/ml, respectively. The results showed that C-PSA-NPs had better uptake profile than curcumin in MCF-7 cell line [40].

3.9. Cell cycle analysis

In order to evaluate the cell cycle effect of prepared formulations on MCF-7 cell line, experiments were conducted using the IC_{50} value of curcumin and C-PSA-NPs (Fig. 7). Curcumin and C-PSA-NPs treated MCF-7 cell line had an increased percentage of cells in G_1 phase compared to untreated control. In particular, higher percentage of cells was observed following C-PSA-NPs treatment (77.3%) and drug alone (76.52%) as compared to control (71.01%). The observed molecular mechanism of curcumin in cell cycle was in agreement with the earlier reports of Srivatsava et al. [46].

3.10. Apoptosis analysis by flow cytometry

The apoptotic profile of curcumin and C-PSA-NPs on MCF-7 cell line was evaluated using flow cytometry after 48 h of exposure. The apoptosis inducing efficiency on MCF-7 cell line was investigated. The percentage population of live cells (bottom left), early apoptotic cells (bottom right), necrotic cells (top left) and late apoptotic cells (top right) are shown in a quadrant in Fig. 8. Cells treated with curcumin showed 1.5%,

13.7% and 44.2% in necrotic stage, late apoptotic stage and early apoptotic stage, respectively. However the C-PSA-NPs treated cells showed lesser number of cells (43.1%) in early apoptotic stage and higher number of cells in both necrotic (1.8%) and late apoptotic stages (16%). The IC_{50} value of curcumin (10.72 μg/ml) and C-PSA-NPs (7 μg/ml) was found with MTT assay. The same IC_{50} concentration was adopted to perform the apoptosis analysis using flow cytometer. So, 7 μg/ml of C-PSA-NPs was able to produce equal percentage of apoptosis as curcumin (10.72 μg/ml). Thus, C-PSA-NPs showed a better apoptotic activity than curcumin. The improved activity of C-PSA-NPs could be due to the better uptake and greater accumulation of nanoparticulate curcumin inside the tumor cells [40].

3.11. High content imaging

The cellular uptake study was evaluated in MCF-7 cell line for curcumin, PSA-NPs and C-PSA-NPs using high content imaging techniques and the results are shown in Fig. 9. C-PSA-NPs localization into the cell was compared with curcumin and the image was taken in bright field and fluorescence images. The merged images will help to predict the localization of C-PSA-NPs. Control cells without the exposure of curcumin and PSA-NPs showed no fluorescence. The C-PSA-NPs treated cells showed nearly a maximum localization of C-PSA-NPs into cells than that of curcumin.

4. Conclusion

Polymer lipid based drug delivery is seen as one of the advancements in drug delivery systems. Through the present study, a novel polymer lipid based nanocarrier delivery system loaded with curcumin has been demonstrated as an effective and potential alternative method for tumor treatment in MCF-7 cell line. The C-PSA-NPs were synthesized using emulsification–solvent evaporation method and 53.2% of curcumin loading was achieved. The hemocompatibility assay also confirmed the biocompatibility of the PSA-NPs with blood cells and the concentration ranges of 60–1200 μg/ml were non-hemolytic. Characterization of the nanocomposite through techniques such as DLS, SEM, FTIR, XRD, and TGA confirmed the ability of C-PSA-NPs as a potential carrier for hydrophobic drug curcumin. A slow and sustained release (%release over a period of 8 days) of curcumin was noted through in vitro release studies. The cell line toxicity by MTT assay, cell cycle and apoptosis studies using flow cytometry showed that C-PSA-NPs had a high apoptotic activity and maximum localization into cells compared with curcumin in MCF-7 cell line. Overall, these findings suggest that C-PSA-NPs may be useful for the treatment of cancer with an improved therapeutic activity of curcumin.

Supplementary data to this article can be found online at http://dx.doi.org/10.1016/j.bbagen.2014.01.016.

Acknowledgements

One of the author SSDK is grateful to CSIR, New Delhi for the SRF fellowship.

References

[1] Y. Liu, H. Miyoshi, M. Nakamura, Nanomedicine for drug delivery and imaging: a promising avenue for cancer therapy and diagnosis using targeted functional nanoparticles, Int. J. Cancer 120 (2007) 2527–2537.
[2] M.S. Muthu, S. Singh, Targeted nanomedicines: effective treatment modalities for cancer, AIDS and brain disorders, Nanomedicine 4 (2009) 105–118.
[3] K.H.A. Hong, Y.-S. Jeon, D.J. Chung, J.-H. Kim, Drug release characteristics of modified PHEMA hydrogel containing thermo-responsive pluronic copolymer, Macromol. Res. 18 (2010) 204–207.
[4] R.B. Chouhan, A.K. Bajpai, An in vitro release study of 5-fluoro-uracil (5-FU) from swellable poly-(2-hydroxyethyl methacrylate) (PHEMA) nanoparticles, J. Mater. Sci. Mater. Med. 20 (2009) 1103–1114.
[5] X. Ma, H. Wang, S. Jin, Y. Wu, X.J. Liang, Construction of paclitaxel-loaded poly(2-hydroxyethyl methacrylate)-g-poly(lactide)-1,2-dipalmitoyl-sn-glycerol-3-phosphoethanolamine copolymer nanoparticle delivery system and evaluation of its anticancer activity, Int. J. Nanomed. 7 (2012) 1313–1328.
[6] F.J. Holly, M.F. Refojo, Wettability of hydrogels. I. Poly(2-hydroxyethyl methacrylate), J. Biomed. Mater. Res. 9 (1975) 315–326.
[7] F. Ayhan, S. Ozkan, Gentamicin release from photopolymerized PEG diacrylate and pHEMA hydrogel discs and their in vitro antimicrobial activities, Drug Deliv. 14 (2007) 433–439.
[8] G.-H. Hsiue, J.-A. Guu, C.-C. Cheng, Poly(2-hydroxyethyl methacrylate) film as a drug delivery system for pilocarpine, Biomaterials 22 (2001) 1763–1769.
[9] R. Chouhan, A.K. Bajpai, Real time in vitro studies of doxorubicin release from PHEMA nanoparticles, J. Nanotechnol. 7 (2009) 5, http://dx.doi.org/10.1186/1477-3155-7-5.
[10] R. Chouhan, A.K. Bajpai, Release dynamics of ciprofloxacin from swellable nanocarriers of poly(2-hydroxyethyl methacrylate): an in vitro study, Nanomedicine 6 (2010) 453–462.
[11] B.V. Slaughter, S.S. Khurshid, O.Z. Fisher, A. Khademhosseini, N.A. Peppas, Hydrogels in regenerative medicine, Adv. Mater. 21 (2009) 3307–3329.
[12] M. Kiremitci, A.I. Serbetci, R. Colak, E. Piskin, Cell attachment to PU and PHEMA based biomaterials: relation to structural properties, Clin. Mater. 8 (1991) 9–16.
[13] A. Mukerjee, J.K. Vishwanatha, Formulation, characterization and evaluation of curcumin-loaded PLGA nanospheres for cancer therapy, Anticancer Res 29 (2009) 3867–3876.
[14] J. Shaikh, D.D. Ankola, V. Beniwal, D. Singh, M.N.V. Ravi Kumar, Nanoparticle encapsulation improves oral bioavailability of curcumin by at least 9-fold when compared to curcumin administered with piperine as absorption enhancer, Eur. J. Pharm. Sci. 37 (2009) 223–230.
[15] M.S. Cartiera, E.C. Ferreira, C. Caputo, M.E. Egan, M.J. Caplan, W.M. Saltzman, Partial correction of cystic fibrosis defects with PLGA nanoparticles encapsulating curcumin, Mol. Pharmaceutics 7 (2009) 86–93.
[16] J. Duan, Y. Zhang, S. Han, Y. Chen, B. Li, M. Liao, W. Chen, X. Deng, J. Zhao, B. Huang, Synthesis and in vitro/in vivo anti-cancer evaluation of curcumin-loaded chitosan/poly(butyl cyanoacrylate) nanoparticles, Int. J. Pharm. 400 (2010) 211–220.
[17] S. Manju, K. Sreenivasan, Conjugation of curcumin onto hyaluronic acid enhances its aqueous solubility and stability, J. Colloid Interface Sci. 359 (2011) 318–325.
[18] N. Suwannateep, W. Banlunara, S.P. Wanichwecharungruang, K. Chiablaem, K. Lirdprapamongkol, J. Svasti, Mucoadhesive curcumin nanospheres: biological activity, adhesion to stomach mucosa and release of curcumin into the circulation, J. Controlled Release 151 (2011) 176–182.
[19] S. Mangalathillam, N.S. Rejinold, A. Nair, V.K. Lakshmanan, S.V. Nair, R. Jayakumar, Curcumin loaded chitin nanogels for skin cancer treatment via the transdermal route, Nanoscale 4 (2012) 239–250.
[20] N.S. Rejinold, M. Muthunarayanan, K.P. Chennazhi, S.V. Nair, R. Jayakumar, Curcumin loaded fibrinogen nanoparticles for cancer drug delivery, J. Biomed. Nanotechnol. 4 (2011) 521–534.
[21] A. Anitha, S. Maya, N. Deepa, K.P. Chennazhi, S.V. Nair, H. Tamura, R. Jayakumar, Efficient water soluble O-carboxymethyl chitosan nanocarrier for the delivery of curcumin to cancer cells, Carbohydr. Polym. 83 (2011) 452–461.
[22] Z. Zheng, X. Zhang, D. Carbo, C. Clark, C.-A. Nathan, Y. Lvov, Sonication-assisted synthesis of polyelectrolyte-coated curcumin nanoparticles, Langmuir 26 (2010) 7679–7681.
[23] T.H. Kim, H.H. Jiang, Y.S. Youn, C.W. Park, K.K. Tak, S. Lee, H. Kim, S. Jon, X. Chen, K.C. Lee, Preparation and characterization of water-soluble albumin-bound curcumin nanoparticles with improved antitumor activity, Int. J. Pharm. 403 (2011) 285–291.
[24] Z. Song, R. Feng, M. Sun, C. Guo, Y. Gao, L. Li, G. Zhai, Curcumin-loaded PLGA–PEG–PLGA triblock copolymeric micelles: preparation, pharmacokinetics and distribution in vivo, J. Colloid Interface Sci. 354 (2010) 116–123.
[25] N.S. Rejinold, M. Muthunarayanan, V.V. Divyarani, P.R. Sreerekha, K.P. Chennazhi, S.V. Nair, H. Tamura, R. Jayakumar, Curcumin-loaded biocompatible thermoresponsive polymeric nanoparticles for cancer drug delivery, J. Colloid Interface Sci. 360 (2011) 39–51.
[26] N.S. Rejinold, P.R. Sreerekha, K.P. Chennazhi, S.V. Nair, R. Jayakumar, Biocompatible, biodegradable and thermo-sensitive chitosan-g-poly(N-isopropylacrylamide) nanocarrier for curcumin drug delivery, Int. J. Biol. Macromol. 49 (2011) 161–172.
[27] S. Maya, M. Sabitha, S.V. Nair, R. Jayakumar, Phytomedicine-loaded polymeric nanomedicines: potential cancer therapeutics, Adv. Polym. Sci. 254 (2013) 203–240.
[28] P. Hu, T. Wang, Q. Xu, Y. Chang, H. Tu, Y. Zheng, J. Zhang, Y. Xu, J. Yang, H. Yuan, F. Hu, X. Zhu, Genotoxicity evaluation of stearic acid grafted chitosan oligosaccharide nanomicelles, Mutat. Res. Genet. Toxicol. Environ. Mutagen. 751 (2013) 116–126.
[29] P. Severino, S.C. Pinho, E.B. Souto, M.H.A. Santana, Polymorphism, crystallinity and hydrophilic–lipophilic balance of stearic acid and stearic acid-capric/caprylic triglyceride matrices for production of stable nanoparticles, Colloids Surf. B Biointerfaces 86 (2011) 125–130.
[30] F.-Q. Hu, S.-P. Jiang, Y.-Z. Du, H. Yuan, Y.-Q. Ye, S. Zeng, Preparation and characterization of stearic acid nanostructured lipid carriers by solvent diffusion method in an aqueous system, Colloids Surf. B Biointerfaces 45 (2005) 167–173.
[31] J. Miao, X.-G. Zhang, Y. Hong, Y.-F. Rao, Q. Li, X.-J. Xie, J.-E. Wo, Inhibition on hepatitis B virus e-gene expression of 10–23 DNAzyme delivered by novel chitosan oligosaccharide-stearic acid micelles, Carbohydr. Polym. 87 (2012) 1342–1347.

[32] Q. Gao, Q. Liang, F. Yu, J. Xu, Q. Zhao, B. Sun, Synthesis and characterization of novel amphiphilic copolymer stearic acid-coupled F127 nanoparticles for nanotechnology based drug delivery system, Colloids Surf. B Biointerfaces 88 (2011) 741–748.
[33] O. Winther-Jensen, R. Vijayaraghavan, J. Sun, B. Winther-Jensen, D.R. MacFarlane, Self polymerising ionic liquid gel, Chem. Commun. (2009) 3041–3043, http://dx.doi.org/10.1039/B822905H.
[34] D.S. Sundar, R. Vijayaraghavan, J. Subramaniam, M. Surianarayanan, A.B. Mandal, Role of choline formate ionic liquid in the polymerization of vinyl and methacrylic monomers, J. Appl. Polym. Sci. 120 (2011) 3733–3739.
[35] E. Lemos-Senna, D. Wouessidjewe, S. Lesieur, D. Duchene, Preparation of amphiphilic cyclodextrin nanospheres using the emulsification solvent evaporation method. Influence of the surfactant on preparation and hydrophobic drug loading, Int. J. Pharm. 170 (1998) 119–128.
[36] L. Liu, L. Sun, Q. Wu, W. Guo, L. Li, Y. Chen, Y. Li, C. Gond, Z. Qian, Y. Wei, Curcumin loaded polymeric micelles inhibit breast tumor growth and spontaneous pulmonary metastasis, Int. J. Pharm. 443 (2013) 175–182.
[37] Y.L. Lin, Y.K. Liu, N.M. Tsai, J.H. Hsieh, C.H. Chen, C.M. Lin, K.W. Liao, A lipo-PEG–PEI complex for encapsulating curcumin that enhances its antitumor effects on curcumin-sensitive and curcumin-resistance cells, Nanomed. Nanotechnol. Biol. Med. 8 (2012) 318–327.
[38] D. Sathish Sundar, M. Surianarayanan, R. Vijayaraghavan, A.B. Mandal, D.R. MacFarlane, Curcumin loaded poly(2-hydroxyethyl methacrylate) nanoparticles from gelled ionic liquids — in vitro cytotoxicity and anti-cancer activity in SKOV-3 cells, Eur. J. Pharm. Sci. 51 (2014) 34–44.
[39] Z. Zhang, S. Dallek, R. Vogt, Y. Li, T.D. Topping, Y. Zhou, J.M. Schoenung, E.J. Lavernia, Degassing behavior of nanostructured Al and its composites, Metall. Mater. Trans. A 41A (2009) 532–541.
[40] C. Mohanty, S.K. Sahoo, The in vitro stability and in vivo pharmacokinetics of curcumin prepared as an aqueous nanoparticulate formulation, Biomaterials 31 (2010) 6597–6611.
[41] S. Karnnet, P. Potiyaraj, V. Pimpan, Preparation and properties of biodegradable stearic acid-modified gelatin films, Polym. Degrad. Stab. 90 (2005) 106–110.
[42] M.M. Yallapu, S.F. Othman, E.T. Curtis, N.A. Bauer, N. Chauhan, D. Kumar, M. Jaggi, S.C. Chauhan, Curcumin-loaded magnetic nanoparticles for breast cancer therapeutics and imaging applications, Int. J. Nanomed. 7 (2012) 1761–1779.
[43] A. Anitha, V.G. Deepagan, V.V. Divya Rani, D. Menon, S.V. Nair, R. Jayakumar, Preparation, characterization, in vitro drug release and biological studies of curcumin loaded dextran sulphate-chitosan nanoparticles, Carbohydr. Polym. 84 (2011) 1158–1164.
[44] M.M. Yellapu, B.K. Gupta, M. Jaggi, S.C. Chauhan, Fabrication of curcumin encapsulated PLGA nanoparticles for improved therapeutic effects in metastatic cancer cells, J. Colloid Interface Sci. 351 (2010) 19–29.
[45] H. Tang, C.J. Murphy, B. Zhang, Y. Shen, E.A. Van Kirk, W.J. Murdoch, M. Radosz, Curcumin polymers as anticancer conjugates, Biomaterials 31 (2010) 7139–7149.
[46] R.K. Srivatsava, Q. Chen, I. Siddiqui, K. Sarva, S. Shankar, Linkage of curcumin-induced cell cycle arrest and apoptosis by cyclin-dependent kinase inhibitor $p21^{/WAF1/CIP1}$, Cell Cycle 6 (2007) 2953–2961.
[47] S.M. Moghimi, A.C. Hunter, J.C. Murray, Long-circulating and target-specific nanoparticles: theory to practice, Pharmacol. Rev. 53 (2001) 283–318.